

## THE PERFORMANCE ANALYSIS OF TOTAL LIGHTNING IN NCAR'S AUTO-NOWCASTER

Nicholas L. Wilson\*  
University of Oklahoma, Norman, Oklahoma

Daniel W. Breed, Cindy K. Mueller, Thomas R. Saxen  
NCAR, Boulder, Colorado

Nicholas W. S. Demetriades  
Vaisala Inc., Tucson, Arizona

### 1. INTRODUCTION

The NCAR Auto-Nowcast (ANC; Mueller et al., 2003) system has now entered its eleventh year of existence. Since its inception in 1995, extensive research has been conducted to improve its convective initiation component. Features have been implemented to detect boundaries via forecaster input and radar-based algorithms. Additionally, infrared satellite cooling is now used to identify areas of instability via cumulus cloud growth (Roberts and Rutledge, 2003) and advanced Rapid Update Cycle-20 km (RUC-20) products such as convergence and maximum 900-700 hPa convective available potential energy (CAPE) (Saxen et al., 2005) have been added recently to improve the ANC's performance. Despite the great advances made in regards to initiation forecasts, the ANC's extrapolation and growth/decay component has remained untouched since 2002, solely using cell trend attributes derived from WSR-88D data. We now introduce total lightning (cloud plus cloud-to-ground) into the ANC's growth/decay fuzzy logic engine to evaluate its performance.

The ANC uses Thunderstorm, Identification, Tracking, Analysis and Nowcasting (TITAN; Dixon and Weiner, 1993) to define contiguous areas of radar reflectivity into individual thunderstorm cells using area and intensity thresholds. TITAN follows the identified thunderstorms in a Lagrangian fashion, calculating various trend attributes for each cell. The robust nature of TITAN allows for easy adaptability toward other Cartesian grid-based datasets such as total lightning by customizing the area and intensity thresholds. In this paper, we detail the method to integrate total lightning into the Dallas-Ft. Worth ANC, share the quantitative results for three archived spring-summer 2005 cases and discuss future issues pertaining toward the use of total lightning in a nowcasting environment.

### 2. DALLAS-FT. WORTH RESEARCH DOMAIN

The ANC was deployed to the Ft. Worth, Texas NWS forecast office in March 2005 as part of the two-year NWS Man In The Loop nowcasting demonstration (Nelson et al., 2005). It is an interactive software package that integrates multiple meteorological datasets in real-time and uses fuzzy logic to combine them and create 60-minute forecasts of thunderstorm, initiation, growth and decay every 5 minutes. The Ft. Worth ANC datasets include: level-II data from 7 WSR-88Ds radars across the southern plains, observed and derived satellite data, METAR and surface mesonet observations, automated feature detection algorithms, a boundary layer model (VDRAS; Sun and Crook, 2001), RUC-20 gridded NWP output and now LDAR II total lightning.

Dallas-Ft. Worth total lightning data have been available in real-time since 2001 from Vaisala Inc.'s second-generation Lightning Detection and Ranging (LDAR II) VHF time-of-arrival 3D mapping network (Demetriades et al., 2002). LDAR II is an array of 7 sensors centered at Dallas-Ft. Worth International Airport with an average radial baseline of 20 to 30 km (Fig. 1). The sensors passively measure radiation emitted by electrical breakdown processes and locate the sources of the radiation to produce 3D mapping of all lightning activity.

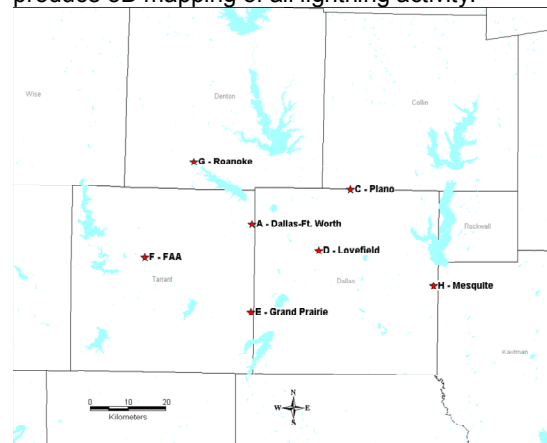


Figure 1. Locations of the Dallas-Ft. Worth LDAR II sites (stars). Sensor A is located at Dallas-Ft. Worth International Airport. Local lakes and county lines are also shown.

\*Corresponding author address: Nicholas L. Wilson, Univ. of Oklahoma, School of Meteorology, SEC 1526, Norman, OK 73071, email: nwilson@ou.edu

### 3. ANC GROWTH/DECAY DATA

Flash Extent Density (FED; Lojou and Cummins, 2005) is used to depict total lightning activity from the LDAR II for applications with the Dallas-Ft. Worth ANC. It employs a “branched segment” reconstruction of the lightning flash using temporal and spatial constraints upon VHF sources created by the electrical breakdown in propagation of mostly negative and some positive leaders. FED helps to normalize the effect of decreasing VHF source detection efficiency with range because flash detection efficiency decreases at a much slower rate with increasing distance from the center of the LDAR II network. Flash detection efficiency is 95% within the network and better than 90% out to a range of 120 km. A 1 km<sup>2</sup> grid box obtains a “hit” if the reconstructed flash passes thru its boundaries. FED was chosen for the ANC because of its similarities in shape, appearance and structure to that of traditional radar reflectivity, allowing for easy implementation of TITAN (Fig. 2).

The LDAR II data are processed in real-time at Vaisala Inc.'s offices in Tucson, Arizona. The FED algorithm is applied to the raw VHF source location information every two minutes and packaged into a NetCDF file with other output. This package is

transmitted to the NWS Southern Region Headquarters in Ft. Worth for dissemination to other outlets (e.g. NWS Ft. Worth forecast office, Ft. Worth CWSU, etc.). For the automated nowcasting purposes of the ANC, it was decided to combine the two-minute FED packages into 4-minute segments. TITAN's cell identification performs better with the added total lightning information provided in 4-minute resolution. Secondly, 4-minute resolution offers improved alignment with the ANC's 5-minute forecast cycle. Lightning cells were identified by TITAN for implementation in the ANC using the minimum 0.25 flashes min<sup>-1</sup> km<sup>-2</sup> (FED) threshold and a 10 km<sup>2</sup> minimum area threshold.

As mentioned earlier, the Dallas-Ft. Worth ANC domain is encompassed by 7 WSR-88D radars. Reflectivity data are updated every 5 to 7 minutes depending on which volume scan strategy is utilized at the time. TITAN is run on a 2.5-tropopause composite reflectivity corrected for brightband contamination. The minimum storm size area used in the ANC for identifying radar reflectivity cells is 10 km<sup>2</sup> and the minimum threshold reflectivity values used are 35 and 45 dBZ.

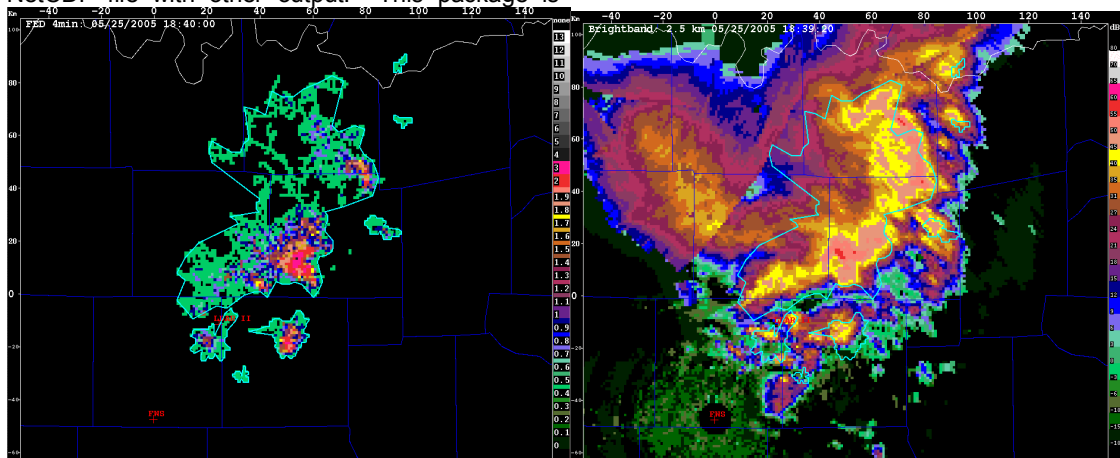


Figure 2. (Left) An example of flash extent density (FED) on 25 May 2005 at 1840 UTC as a squall line moves southeast across the Dallas-Ft. Worth area. The TITAN-identified total lightning cell boundary is displayed in cyan. The color-bar on the right depicts the units for FED: flashes min<sup>-1</sup> km<sup>-2</sup>. The cross represents the location of the KFWS WSR-88D in southern Tarrant Co. (Right) An example of 2.5 km radar reflectivity CAPPI for the same event at 1839 UTC with the total lightning cell overlaid in cyan. The color-bar on the right depicts the units for radar reflectivity: dBZ.

### 4. ANC GROWTH/DECAY MEMBERSHIP FUNCTIONS

#### 4.1 Radar Reflectivity-derived

The purpose of the ANC growth/decay component is to predict whether a TITAN 35 dBZ threshold storm cell will grow, maintain its current area or dissipate 60 minutes from the forecast time. The most effective TITAN-derived radar reflectivity thunderstorm cell attribute for this task is the history-weighted normalized area growth rate

(NAGR). The NAGR takes into account the last five sets of data, thus the past 25 to 30 minutes of radar information is used to predict the future trend of cell growth and decay. The other TITAN-derived attribute used by the ANC is the maximum reflectivity found within the boundaries of the identified cell. Boundary relative steering flow (Wilson and Megenhardt, 1997) is used as well, with weaker winds more conducive toward cell growth.

The key components of any fuzzy logic based system are the membership functions. A membership function defines the “degree of

truthness” of a certain parameter. The ANC is the ideal framework to use fuzzy logic with its multiple datasets and the non-binary decision making necessary to make meteorological forecasts. The growth/decay component of the ANC uses membership functions weighted from -1 to 1 for TITAN-derived cell attributes. Negative values indicate cell decay, values near 0 indicate maintenance of cell area and values near 1 indicate cell growth. Examples of the current membership functions used in the growth/decay component of the ANC are found below (Fig. 3-6).

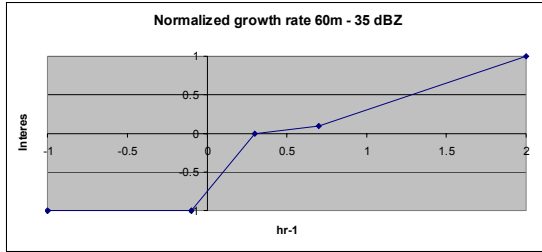


Figure 3. ANC membership function for the TITAN-derived 35 dBZ threshold cell normalized area growth rate.

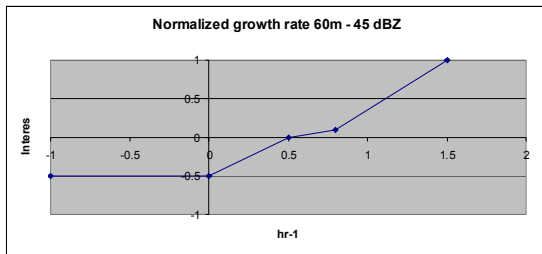


Figure 4. Same as Figure 3, except now for the TITAN-derived 45 dBZ threshold.

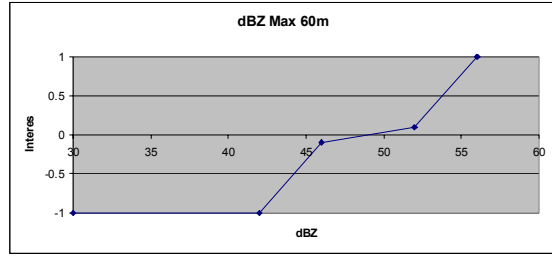


Figure 5. ANC membership function for the TITAN-derived maximum value of reflectivity in a cell.

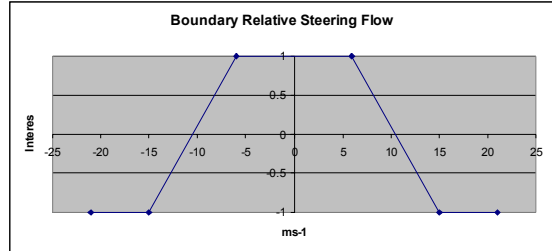


Figure 6. ANC membership function for the boundary relative steering flow.

#### 4.2 Total Lightning-derived

The success of using TITAN to identify total lightning cells provides confidence that similar attributes discussed in Section 4.1 will be applicable to trends in FED. With this in mind, total lightning membership functions have been developed that are analogous to those derived from radar reflectivity. The total lightning membership functions have been conditioned using the analysis of 15 thunderstorm cells over six different convective weather events that traversed the Dallas-Ft. Worth area (Table 1).

Date	Cell ID	Initiation or Domain Entry Time (UTC)	Dissipation or Domain Exit Time (UTC)	Synoptic Mode of Convection
5-Apr	Dallas Co. I	2210	0235	Squall Line
25-Apr	Central	1930	0000	Supercell
25-Apr	Northern	1930	2220	Supercell
25-Apr	Southern	1925	0130	Supercell
25-May	Isolated	1920	2100	Squall Line
25-May	Main Line	1600	2215	Squall Line
25-May	Tail-End	1810	2145	Squall Line
14-Jun	Eastern	0220	0630	Multicell
14-Jun	Eastern Isolated	0530	0920	Multicell
14-Jun	Western	0400	0925	Multicell
1-Jul	Eastern Merge	1410	2000	MCS
1-Jul	Western Merge	1545	2000	MCS
11-Jul	Dallas Co. II	2120	0110	Isolated
11-Jul	N Tarrant Co.	1915	2030	Isolated
11-Jul	NW Tarrant Co.	1935	2100	Isolated

Table 1. A listing of the 15 individual convective cells used to condition the total lightning membership functions for use in the ANC. The first column depicts the date of the event and the second column specifies the thunderstorm ID. The third column provides the initiation or domain entry time (in UTC) and the fourth column provides the dissipation or domain exit time (in UTC) of the respective thunderstorm cell. The fifth column describes the predominant convective mode of the event day.

Two total lightning membership functions from TITAN-derived attributes have been developed for testing in the ANC. The first is the 0.25 FED threshold history-weighted NAGR (Fig. 7). Similar to the radar reflectivity NAGRs, the total lightning NAGR takes into account the last five sets of data, thus using 20 minutes of information due to its 4-minute temporal resolution. The other total lightning membership function that has been developed is the maximum FED value (Fig. 8). Each of these membership functions have been formulated using forecast skill score analysis across the 15 training cases to optimize their growth/decay inflection point. NAGR values above  $0.5 \text{ hr}^{-1}$  and maximum FED values above  $2.5 \text{ flashes min}^{-1} \text{ km}^{-2}$  indicate cell growth. The method to combine these membership functions into a thunderstorm cell growth/decay forecast tool is detailed in the next section.

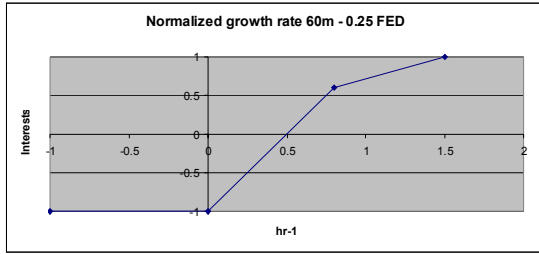


Figure 7. ANC membership function for the TITAN-derived 0.25 FED threshold cell normalized area growth rate.

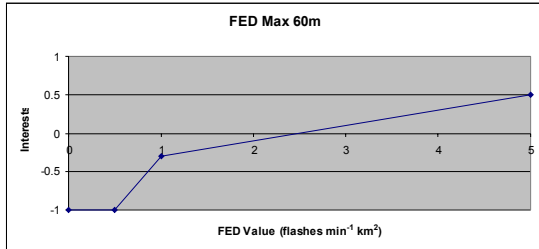


Figure 8. ANC membership function for the TITAN-derived maximum value of FED in a cell.

## 5. ANC GROWTH/DECAY FUZZY LOGIC SCHEME

The membership functions presented in Section 4 are the building blocks for the growth/decay forecast output by the ANC. At every ANC forecast period (typically 5 minutes), the TITAN-derived attributes are calculated for each identified cell. The TITAN attribute value is then converted to an interest value using its predefined membership function. These unitless interest fields can be displayed graphically within the ANC for the forecasters' use and are known as likelihood fields. Next, the interest values are multiplied by a certain weighting depending on their importance (Table 2). The total lightning membership function weights have been chosen subjectively to balance their radar reflectivity counterparts. Finally, the weighted

interest values are summed and final conditions are applied to the TITAN-identified cell of interest (Table 3). TITAN extrapolates the cell using cross-correlation techniques and contracts, maintains or expands its boundaries according to the final conditions.

Membership Function	Weight	Interest Value Range	Weighted Interest Value Range
Boundary Relative Steering Flow	0.21	-1 to 1	-0.21 to 0.21
35 dBZ NAGR	0.30	-1 to 1	-0.3 to 0.3
45 dBZ NAGR	0.15	-0.5 to 1	-0.075 to 0.15
Maximum dBZ	0.20	-1 to 1	-0.20 to 0.20
0.25 FED NAGR	0.30	-1 to 1	-0.30 to 0.30
Maximum FED	0.20	-1 to 0.5	-0.20 to 0.10

Table 2. A detailed list of the ANC membership functions used. The first column provides the name of the membership function. The second column lists the weighting given to the membership function and the third column lists the range of the membership function's interest values. The fourth column provides the weighted interest value ranges for each membership function that contribute to the final growth/decay forecast.

Range of Summed Interest Values	TITAN Growth (+) / Decay (-) of Cell Boundaries
-100 to -0.7	-6 km
-0.7 to -0.5	-4 km
-0.5 to -0.3	-2 km
-0.3 to -0.2	-1 km
-0.2 to 0.2	0 km
0.2 to 0.3	+1 km
0.3 to 0.5	+2 km
0.5 to 0.7	+3 km
0.7 to 0.9	+5 km
0.9 to 99	+7 km

Table 3. The final conditions applied to the summation of weighted interest values for the ANC's growth/decay component. The first column provides the range values and the second column lists the resultant 60-minute forecast for expansion, maintenance or contraction of the TITAN 35 dBZ cell boundaries.

## 6. RESULTS

Three archived Dallas-Ft. Worth ANC cases were identified to evaluate the performance of its growth/decay forecast logic with and without total lightning membership functions. 60-minute forecasts by the ANC using its current growth/decay component and the ANC with the addition of total lightning fields (herein thereafter "ANC-LTG") are compared in the following cases.

Grid-based quantitative performance analysis is conducted for each case using the following traditional indices: probability of detection (POD), false alarm ratio (FAR) and critical success index (CSI).

- $POD = Hits / (Hits + Misses)$
- $FAR = False\ Alarms / (Hits + False\ Alarms)$
- $CSI = Hits / (Hits + Misses + False\ Alarms)$

Detailed results for the three cases can be found in Table 4.

### 6.1 25 April 2005

Several supercell thunderstorms developed along and ahead of a cold front and dryline on this day in late April. Deep layer (0-6 km) shear was strong (around 50 kts) and the shear vector was nearly perpendicular to the dryline. The most significant supercells developed in Tarrant and Johnson Counties (Fig. 9) and moved east-southeast. The Tarrant County storm produced two brief FO tornado touchdowns near or just west of Mansfield and near Cedar Hill at 2135 UTC. This supercell was also responsible for the most intense total lightning activity observed by LDAR II since its installation. Peak values of 31.5 flashes  $min^{-1} km^{-2}$  were observed at both 2136 UTC and 2146 UTC, along with radar reflectivity values up to 71.5 dBZ. The Tarrant supercell storm eventually weakened as it moved across extreme southern Dallas County. The Johnson County supercell also produced a brief FO tornado near Maypearl in Ellis County at 2200 UTC with peak FED values of 16.5 flashes  $min^{-1} km^{-2}$ . Other severe storms affected parts of Grayson, Fannin, Hunt, Delta, and Hopkins Counties through the evening with hail reports up to 2.00 inches. An example ANC forecast and subsequent verification for the event are seen to the right (Fig. 10-11).

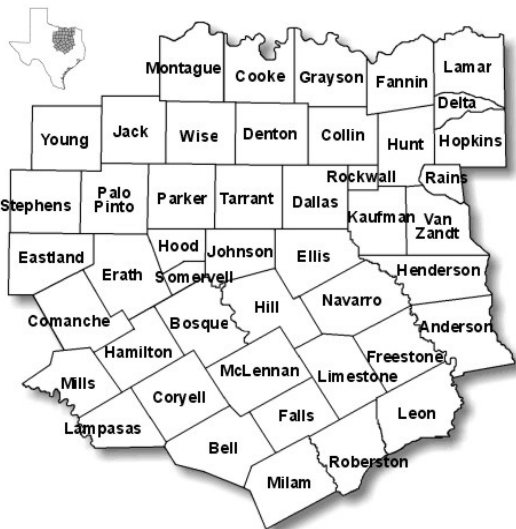


Figure 9. A detailed map of the area and counties encompassed by the NWS Ft. Worth forecast office county warning area (CWA).

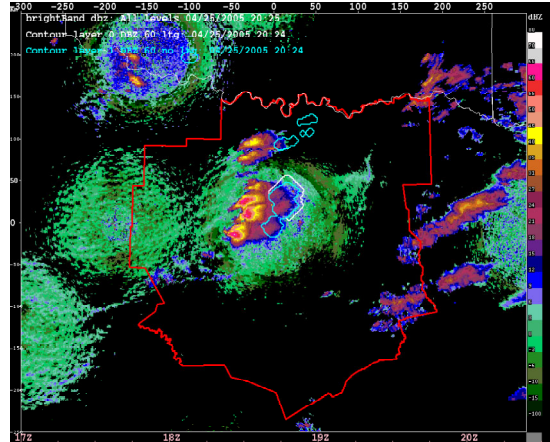


Figure 10. The 60-minute ANC forecast output on 25 April 2005 at 2024 UTC. The cyan boundaries are the forecasted 35 dBZ threshold cell position in 60 minutes using the current ANC growth/decay scheme. The white boundary is the forecasted 35 dBZ threshold cell position in 60 minutes using the ANC-LTG scheme with total lightning (ANC-LTG). The red boundary represents the NWS Ft. Worth forecast office county warning area.

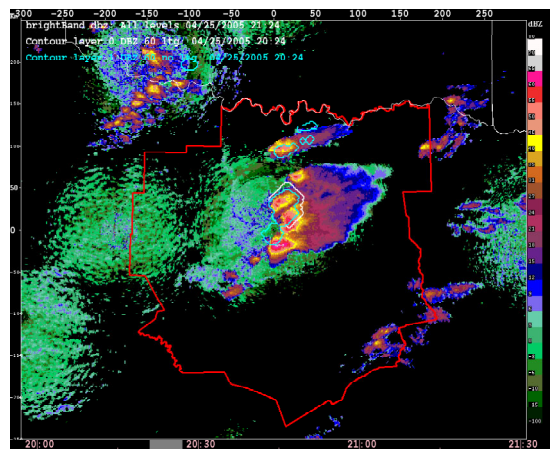


Figure 11. The 60-minute 2024 UTC forecast verification at 2124 UTC on 25 April 2005. The cyan boundaries are the forecasted 35 dB Z threshold cells using the current ANC growth/decay scheme. The white boundaries are the forecasted 35 dBZ threshold cells using the ANC-LTG. The red boundary represents the NWS Ft. Worth forecast office county warning area. Cell growth and extrapolation are well captured in this example.

The ANC-LTG re-analysis demonstrates mixed results in the re-analysis of this particular event. Its average POD provides an encouraging 2.31% improvement in overall performance (Table 4). The increased POD is especially noticeable between the 2105 to 2253 UTC verification times, but the FAR also rises at this time (Fig. 12-13). Although TITAN 35 dBZ threshold cells initiated at 1923 UTC, FED cells did not initiate until 2005 UTC due to extensive warm-precipitation processes that dominated the early lifecycle of the supercells as discussed in Wilson et al. 2005. Similar to the POD, the ANC-LTG's CSI begins outperforming the

current ANC set-up during the latter stages of the supercells' growth at 2105 UTC verification time (Fig. 14).

The increased FAR values for this case are partially explained by poor LDAR II network performance in vicinity of the Johnson County supercell. For instance, maximum reflectivity values of 72 dBZ were only accompanied by maximum FED values of 3 flashes  $\text{min}^{-1} \text{km}^2$  at 2240 UTC. It is likely that a combination of unique microphysical processes associated with the supercell's hail production and VHF signal attenuation hampered the identification of source locations, subsequently corrupting the TITAN-derived 0.25 threshold FED cell trends.

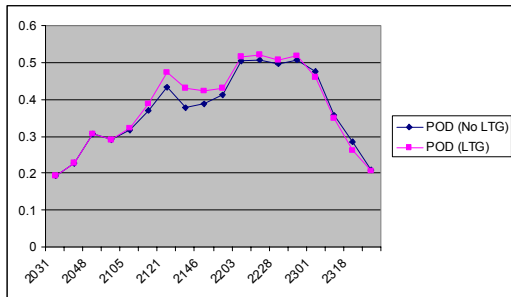


Figure 12. The 25 April 2005 time-series (in UTC) POD for the ANC's current forecast logic (blue) and the ANC-LTG (pink).

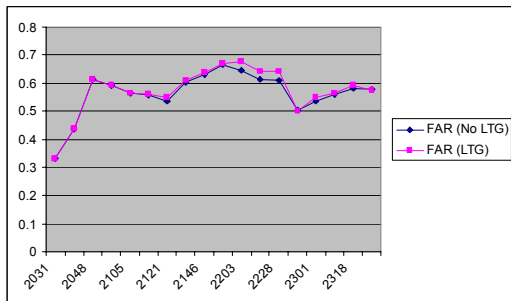


Figure 13. Same as Figure 12, except now for the FAR.

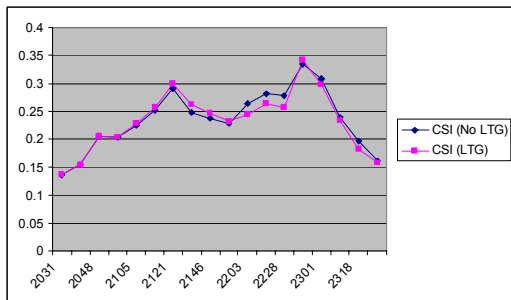


Figure 14. Same as Figure 12, except now for the CSI.

## 6.2 25 May 2005

A squall line approached the Dallas-Ft. Worth area from the northwest on this day at 1600 UTC. CAPE vales near  $800 \text{ J kg}^{-1}$  and 30 kt steering flow characterized the event. Moderate lightning activity

accompanied these non-severe thunderstorms as they passed through Dallas County. Peak total lightning activity up to  $11 \text{ flashes min}^{-1} \text{km}^{-2}$  was observed in the main line at 1910 UTC. Additional isolated convective cells developed on the southern flank of the squall line around 1900 UTC. Moderate lightning activity of  $8.25 \text{ flashes min}^{-1} \text{km}^{-2}$  accompanied a cell to the south of Dallas at 1910 UTC before it weakened considerably. The squall line and associated convective cells departed the NWS Ft. Worth CWA by 2200 UTC. An example of the ANC forecast output and subsequent verification are provided below (Fig. 15-16).

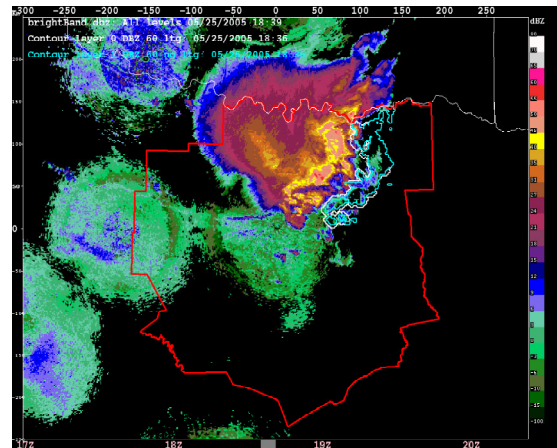


Figure 15. Same as Figure 10, except now the ANC 60-minute forecast output on 25 May 2005 at 1836 UTC.

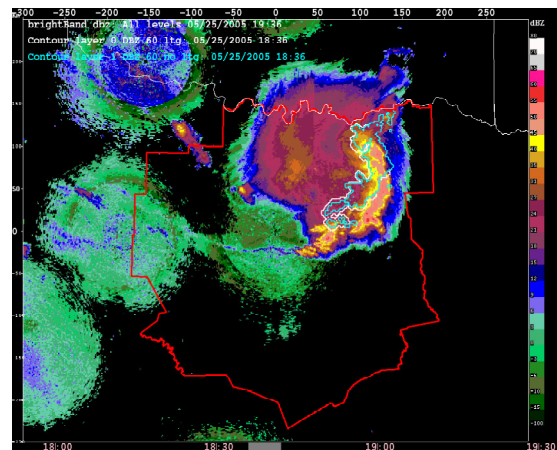


Figure 16. Same as Figure 11, except now the 60-minute 1836 UTC forecast verification at 1936 UTC on 25 May 2005. Cell growth is well captured in this example, but errors in the extrapolation significantly deteriorated the forecast skill scores at this time.

The ANC-LTG provides significant improvement in the POD from 1911 UTC to 2116 UTC (Fig. 17). Despite the overall poor performance of the ANC during the latter stages of this case, the ANC-LTG slightly improves the FAR scores 10 out of 11 forecast periods between 1821 UTC and 1953 UTC (Fig. 18). During the decay stages of the multicell event, the ANC-LTG

improved the POD by 9.40%, reduced the FAR by 0.91% and increased the CSI by 2.98% (Fig. 19). The largest source of error leading to CSI values below 0.15 during the decay stage of this case was TITAN's poor extrapolation of the 35 dBZ cells. We emphasize the importance of focusing on the relative improvement of the ANC with total lightning fields, as opposed to the raw quantitative numbers. Acceleration of the squall line's southern flank in the example shown (Fig. 15-16) led to poor performance in the forecast verification scores at and around 1936 UTC. New object-based verification techniques (Halley-Gotway et al., 2005) will alleviate these ANC forecast evaluation problems in the near future.

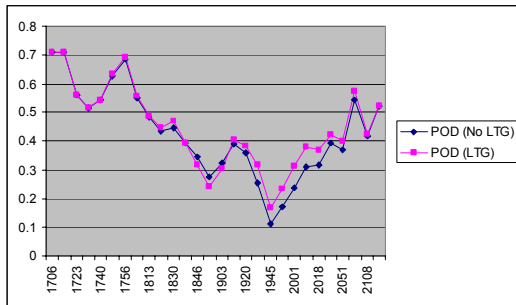


Figure 17. The 25 May 2005 time-series (in UTC) POD for the ANC's current forecast logic (blue) and the ANC-LTG (pink).

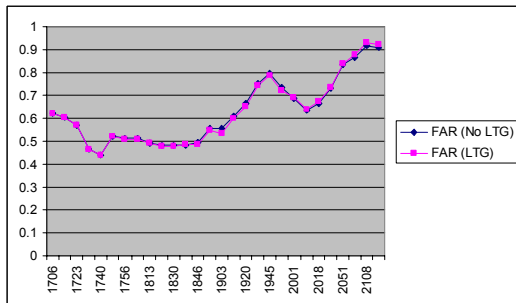


Figure 18. Same as Figure 17, except now for FAR.

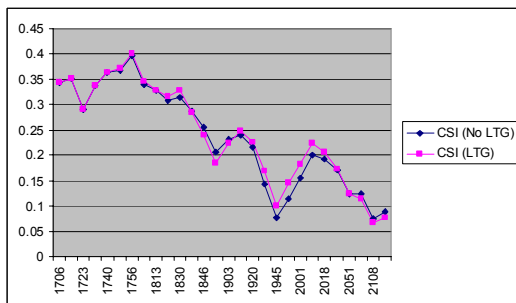


Figure 19. Same as Figure 17, except now for the CSI.

### 6.3 1 July 2005

Two large non-severe multicell complexes propagated southward across the Dallas-Ft. Worth area on this day, finally merging in eastern Johnson

County at 1800 UTC. CAPE values exceeded  $1000 \text{ J kg}^{-1}$  and strong low-level directional shear were present during the mid-afternoon. The easternmost multicell complex was characterized by intense lightning activity, with FED values as high as  $17.75 \text{ flashes min}^{-1} \text{ km}^{-2}$  in Dallas County at 1740 UTC. A brief jump in lightning activity from 9 to 13 flashes  $\text{min}^{-1} \text{ km}^{-2}$  was witnessed after the two complexes merged together at 1805 UTC, but large-scale decay began shortly thereafter. By 2000 UTC, total lightning activity had ceased and the maximum radar reflectivity had weakened below 35 dBZ. An example of the ANC forecast output and subsequent verification are provided below (Fig. 20-21).

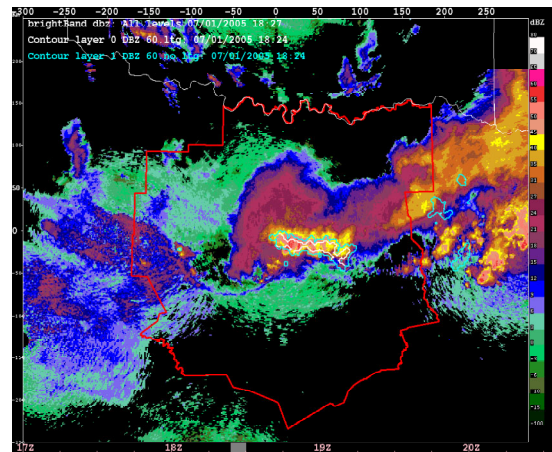


Figure 20. Same as Figure 10, except now the ANC 60-minute forecast output on 1 July 2005 at 1824 UTC.

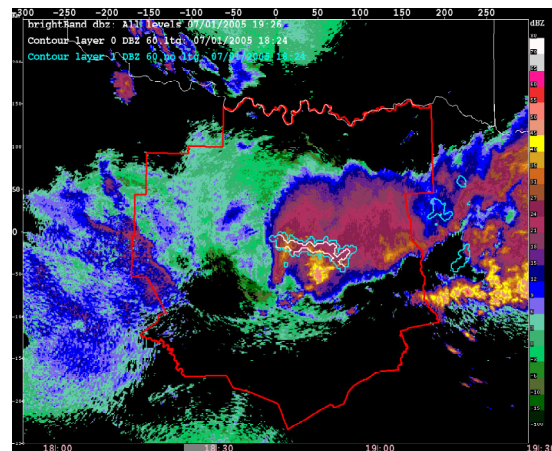


Figure 21. Same as Figure 11, except now the 60-minute 1824 UTC forecast verification at 1926 UTC on 1 July 2005. Cell decay is well captured in this example, although the poor extrapolation forecast is once again responsible for deteriorating the forecast skill scores.

The ANC-LTG provides slight overall improvement to the POD, FAR and CSI in this case (Fig. 22-24). The total lightning membership functions perform exceptionally well during the mature stage of the event, with a 5.27% improvement in POD, a 1.13% reduction in FAR

and 4.42% increase in CSI (Table 4). However, the performance during the decay of the multicell complex was somewhat disappointing with poorer results in all of the forecast skill scores. During the analyzed 1800 to 2000 UTC time period while decay is ongoing, the multicell complex drifted to the south of the Dallas-Ft. Worth area toward Hill and Navarro Counties. This is a considerable distance from the southernmost LDAR II sensor at Grand Prairie (Fig. 1), leading to degradation in VHF source detection and reconstruction of flashes necessary for FED. It is likely that the range constraints of LDAR II decrease the ability of TITAN-derived total lightning cell attributes to accurately capture trends in thunderstorm growth/decay in these instances

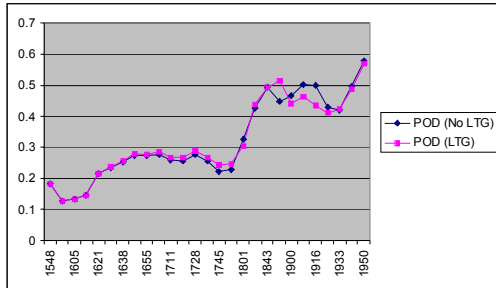


Figure 22. The 1 July 2005 time-series (in UTC) POD for the ANC's current forecast logic (blue) and the ANC-LTG (pink).

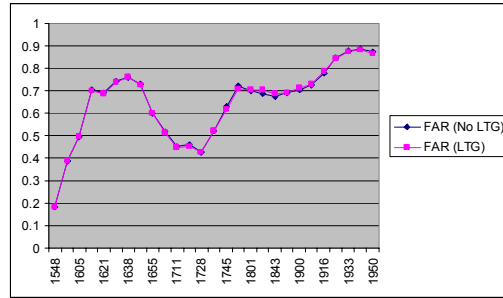


Figure 23. Same as Figure 22, except now for the FAR.

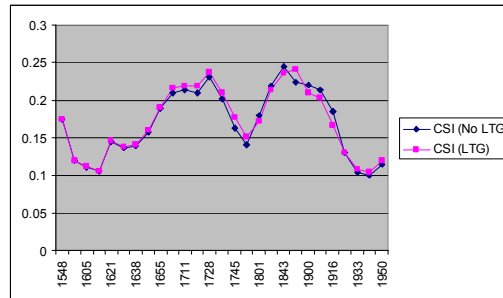


Figure 24. Same as Figure 22, except now for the CSI.

Event and Storm lifecycle stage	ANC current set-up	ANC-LTG	Change (in %)	ANC current set-up	ANC-LTG	Change (in %)	ANC current set-up	ANC-LTG	Change (in %)
	POD	POD		FAR	FAR		CSI	CSI	
<b>25-Apr</b>									
<b>Overall</b>	<b>0.37021</b>	<b>0.37878</b>	<b>+2.31</b>	<b>0.56406</b>	<b>0.57225</b>	<b>-1.45</b>	<b>0.23549</b>	<b>0.23346</b>	<b>-0.86</b>
Growth	0.30520	0.31411	+2.89	0.51784	0.52048	-0.51	0.20934	0.21182	+1.19
Mature	0.41152	0.41992	+2.04	0.59348	0.60519	-1.97	0.25213	0.24723	-1.94
Decay	N/A	N/A	N/A	N/A	N/A	N/A	N/A	N/A	N/A
<b>25-May</b>									
<b>Overall</b>	<b>0.42823</b>	<b>0.44571</b>	<b>+4.08</b>	<b>0.62834</b>	<b>0.62678</b>	<b>+0.25</b>	<b>0.23731</b>	<b>0.2416</b>	<b>+1.81</b>
Growth	0.58137	0.58534	+0.68	0.52166	0.52090	+0.15	0.34293	0.34493	+0.58
Mature	0.30676	0.32253	+5.14	0.61297	0.60370	+1.51	0.20836	0.21501	+3.19
Decay	0.38863	0.42514	+9.40	0.78088	0.78798	+0.91	0.14147	0.14568	+2.98
<b>1-Jul</b>									
<b>Overall</b>	<b>0.32202</b>	<b>0.32218</b>	<b>+0.05</b>	<b>0.64681</b>	<b>0.64646</b>	<b>+0.05</b>	<b>0.17002</b>	<b>0.17140</b>	<b>+0.81</b>
Growth	0.20473	0.20658	+0.91	0.58773	0.58672	+0.17	0.14221	0.14327	+0.75
Mature	0.25342	0.26678	+5.27	0.52374	0.52673	+1.13	0.19578	0.20442	+4.42
Decay	0.46165	0.45201	-2.09	0.76774	0.77154	-0.49	0.17638	0.17341	-1.69

Table 4. A detailed analysis of the ANC 60-minute forecast skill scores. The first column lists the event date and below that the skill scores are divided into four storm lifecycle sub-sets: Overall – average of every forecast for the entire event, Growth – forecasts as aerial coverage increased, Mature – forecasts at and around the peak of aerial storm coverage and Decay – forecasts as the aerial decreased. The orange colored columns compare the ANC's current growth/decay forecast POD performance to that of the ANC-LTG. The fourth column describes the percentage improvement (+) or degradation (-) in the skill score when using the ANC with total lightning. The yellow and blue columns are the same, analyzing FAR and CSI respectively.



## 7. DISCUSSION AND FUTURE WORK

The addition of total lightning to the Dallas-Ft. Worth ANC growth/decay forecast logic demonstrates the potential for improved 60-minute nowcasting performance. In our three case studies, the ANC-LTG increased the POD by over 2% on average. The FAR was decreased slightly and the CSI improved by over 0.8% in two of the three cases. The fuzzy logic scheme used with the total lightning for this study was conservative, so it is expected that emphasizing more weight upon the TITAN-derived FED membership functions would further improve 60-minute growth/decay forecasting performance in most instances. Additional case studies should be analyzed to better understand the effects of the total lightning membership functions upon the complex growth/decay forecast component of the ANC. Adjustments to the fuzzy logic weighting and final growth/decay constraints could offer substantially different results. There may also be a total lightning dependence upon mode of convection and performance.

As seen with the advancement of the ANC's convective initiation component, additional membership functions provide redundancy in the fuzzy logic, and in turn improve ANC forecast output. It is recommended that future evolution of the ANC growth/decay component include radar reflectivity and total lightning derived membership functions when available. Short-term mesoscale NWP and mesonet surface observations should also be considered possible growth/decay forecast components to obtain a better grasp of the in-situ and future environment of ongoing convection, as opposed to the history-weighted trends currently used.

Extrapolation is the most significant source of error in the 60-minute forecast output provided by the ANC. It may be possible to improve the TITAN 35 dBZ threshold cell motion vectors using the cross-correlation of total lightning cells. However, this introduces other difficulties such as how to handle cells with warm-precipitation processes that lack lightning activity and the range limitations of the LDAR II network. Continued advancement of the ANC's VDRAS boundary-layer model may also provide added benefit toward the extrapolation forecasts with its potential for real-time tropospheric wind analysis in the future.

The integration of LDAR II data into the Dallas-Ft. Worth ANC has shown that total lightning's nowcasting skill is at least on par with WSR-88D radar reflectivity during most scenarios in close proximity (within 100 km) to the network. The next step for NCAR will be the introduction of total lightning into the new ANC forecast demonstration project at White Sands Missile Range (WSMR) in New Mexico. This region is characterized by isolated and electrically active convection. Similar methods discussed in this paper will be utilized to integrate data from the WSMR total lightning

mapping array into its ANC installation; with hopes to improve the 0-to-60 minute growth/decay forecast performance.

*Acknowledgements:* The National Center for Atmospheric Research is sponsored by the National Science Foundation. This study is supported by funding from Vaisala Inc. and the U.S. Army Test and Evaluation Command.

## 8. REFERENCES

Demetriades, N. W. S., M. J. Murphy, and K. L. Cummins, 2002: Early results from the Global Atmospheric, Inc. Dallas-Ft. Worth lightning detection and ranging (LDAR-II) research network. Preprints, *6<sup>th</sup> Symposium on Integrated Observing Systems*, Orlando, FL, Amer. Meteor. Soc., 202-209.

Dixon, M., and G. Wiener, 1993: TITAN: Thunderstorm Identification, Tracking, Analysis, and Nowcasting—A radar-based methodology. *J. Atmos. Oceanic Technol.*, **10**, 785–797.

Halley-Gotway, J., R. Bullock, B. Brown, 2005: Object-based verification of convective storms for the 2005 Dallas/Ft. Worth AutoNowcaster Demonstration Project. Preprints, *32<sup>nd</sup> Conference on Radar Meteorology*, Albuquerque, NM, AMS.

Lojou, J. Y., and K. L. Cummins, 2005: On the representation of two- and three-dimensional total lightning information. AMS Preprints, *1<sup>st</sup> Conference on Meteorological Applications of Lightning Data*, San Diego, CA, Amer. Meteor. Soc., 7pp.

Mueller, C., T. Saxen, R. Roberts, J. Wilson, T. Betancourt, S. Dettling, N. Oien, and J. Yee, 2003: NCAR Auto-Nowcast System. *Wea. Forecasting.*, **18**, 545-561.

Nelson, E. J., S. J. Fano, R. Roberts, W. Bunting, T. Saxen, C. Mueller, H. Cai, A. Crook, D. Megenhardt, and J. Pinto. Evaluation of the NCAR Thunderstorm Auto-Nowcaster during the NWS Ft. Worth Operational Demonstration. Preprints, *32<sup>nd</sup> Conference on Radar Meteorology*, Albuquerque, NM, Amer. Meteor. Soc.

Roberts, R. D., and S. Rutledge, 2003: Nowcasting Storm Initiation and Growth Using GOES-8 and WSR-88D Data. *Wea. Forecasting.*, **18**, 562-584.

Saxen, T. R., C. K. Mueller, N. A. Rehak, 2005: Determining key predictors for NCAR's convective Auto-Nowcast System using climatological analyses. Preprints, *32<sup>nd</sup> Conference on Radar Meteorology*, Albuquerque, NM, Amer. Meteor. Soc.

Sun, J., and N. A. Crook, 2001: Real-time low-level wind and temperature analysis using WSR-88D data. *Wea. Forecasting.*, **16**, 117–132.

Wilson, J. W., and D. L. Meegenhardt, 1997: Thunderstorm initiation, organization, and lifetime associated with Florida boundary layer convergence lines. *Mon. Wea. Rev.*, **125**, 1507–1525.

Wilson, N. L., D. W. Breed, T. R. Saxen, and N. W. S. Demetriades, 2005: The complementary use of TITAN-derived radar and total lightning cells. Preprints, *32<sup>nd</sup> Conference on Radar Meteorology*, Albuquerque, NM, Amer. Meteor. Soc.